International Conference on Nuclear Data for Science and Technology 2007
DOI: 10.1051/ndata:07186

Production of carrier-free ^{28}Mg by 50–200 MeV protons on ^{nat}Cl: excitation function and target optimization

G.F. Steyn[a], N.P. van der Meulen, T.N. van der Walt, and C. Vermeulen

iThemba Laboratory for Accelerator Based Sciences, P.O. Box 722, Somerset West 7129, South Africa

Abstract. Thick-target production rates and excitation function data are presented for ^{28}Mg formed in the proton irradiation of ^{nat}Cl up to 200 MeV. The results are compared with previous literature experimental data, where available. Various compounds were investigated for their suitability as target materials. A practical target geometry utilizing encapsulated LiCl discs is suggested.

1 Introduction

The only feasible radiotracer of Mg is the β^--emitter ^{28}Mg (half-life 20.9 h), as all the other Mg radionuclides have half-lives shorter than 10 minutes. Since its introduction *circa* 1952 as a radiotracer in biochemical studies [1], ^{28}Mg found wide application in the study of absorption, retention and excretion in metabolic processes in animals and humans [2–4]. Magnesium is the second most abundant soft tissue intracellular cation in vertebrates and an essential nutrient for all living organisms. As such, ^{28}Mg played an important role in studies of Mg bioavailability in agriculture and nutrition (e.g., [5,6]).

The general availability of no-carrier-added ^{28}Mg has, however, remained limited as rather low yields are obtained from all feasible production methods. In addition, the rather short half-life of 20.9 h limits its usefulness as a tracer to only about three days. Stable tracers are, therefore, more commonly used nowadays, especially in studies of processes having relatively long biological half-lives. In spite of this, the simultaneous administration of ^{28}Mg with a stable Mg tracer remains useful for monitoring the initial Mg uptake and to evaluate the stable tracer technique [4].

With nuclear reactors, ^{28}Mg can be produced by neutron irradiation of Li-Mg alloy targets, utilizing the consecutive reactions ^{6}Li(n,t)^{4}He and ^{26}Mg(t,p)^{28}Mg (e.g., Kolar et al. [7]). Unfortunately, in addition to a low yield, the product is not carrier free. At a few high-energy accelerators, the production of ^{28}Mg utilizing spallation reactions have been demonstrated (e.g., [8]). In addition to a low yield, extensive radiochemical purification is required to obtain a radionuclidically pure product as spallation reactions produce a mixture of many elemental species. At a few smaller facilities, routine production programmes existed for some time utilizing the ^{27}Al(α,3p)^{28}Mg reaction [9] (e.g., FZ-Jülich, Germany [10]), suitable for producing small to moderate quantities. Nowadays, however, α-particle beams for radionuclide production purposes are becoming extremely rare, as most modern medical cyclotrons are negative ion accelerators. With protons, beam energies well above 50 MeV are required as all the feasible (p,ypxn) reactions have relatively high reaction thresholds. The production of ^{28}Mg, therefore, falls outside the domain of most commercial medical cyclotrons. A number of larger accelerators, however, do have the ability to produce useful quantities of ^{28}Mg using proton beams.

The present investigation revisits the options available for ^{28}Mg production in the proton energy region 50–200 MeV. Extensive new production rate and excitation function data are presented for the ^{nat}Cl(p,6pxn)^{28}Mg nuclear process.

2 Experimental methods and data analysis

Usually, excitation functions are measured utilizing the well-known stacked-foil technique; the foils being sufficiently thin to ensure that the measured cross sections constitute microscopic data. From these microscopic data, production rates or yields can be deduced by means of a numerical integration procedure [11].

Occasionally, however, it is difficult to use the stacked-foil technique due to difficulties in preparing thin specimens of high integrity of a given material. This was experienced with the stable compounds of Cl, the chlorides being brittle salts. Thick-target yields were, therefore, measured in a range of different energy windows, using relatively thick NaCl discs as targets, in order to establish the thick-target production rate curve first. The corresponding excitation function was then deduced by means of a differentiation procedure, in order to obtain microscopic data for comparison with other measured cross sections in the literature. An important criterion of this approach is that the spacing of the measured points on the energy axis should be similar to what would have been appropriate in a conventional stacked-foil experiment.

Stacks of analytical grade NaCl (>99%, Merck) tablets were irradiated with proton beams of nominally 200, 100 and 66 MeV, delivered by the separated sector cyclotron of iThemba LABS. The NaCl target discs had thicknesses of nominally 870, 540 and 425 mg/cm^2, respectively, in the 200, 100 and 66 MeV stacks. The individual NaCl discs were separated by relatively thin monitor foils (99.9%, Goodfellow, U.K.): 65 mg/cm^2 Al in the 200 and 100 MeV stacks and 44 mg/cm^2 Cu in the 66 MeV stack. The excitation functions of the ^{22}Na and ^{65}Zn formed in the Al and Cu foils, respectively, were used to monitor the accumulated proton charge.

[a] Presenting author, e-mail: Deon@tlabs.ac.za

These well-established monitor reactions, recommended by the IAEA [12], gave consistent results with the readings of a calibrated Brookhaven Instruments Corporation Model 1000C current integrator.

The ^{28}Mg activities were determined by off-line γ-ray spectrometry using the 941.7 keV (38.3%) and 1342.3 keV (52.6%) γ-lines [13]. The ^{28}Mg sources were prepared by dissolving each NaCl tablet in 10 ml of water after irradiation. These solutions were sealed in standard serum vials. An accurately calibrated HPGe detector with a relative efficiency of 13% and a resolution of 1.8 keV at 1.33 MeV, connected to a Silena EMCAPLUS multi-channel analyser, was used for all activity measurements. The thick-target production rate curve was obtained by summing the individual ^{28}Mg activities progressively. Corrections were made for the missing ^{28}Mg activities corresponding to the "dead layer" energy intervals occupied by the monitor foils. This was done by interpolating the activity values on both sides of each dead layer and scaling to include the full energy region.

The total uncertainties of the measured activity values were obtained by summing all the contributing uncertainties in quadrature and are expressed with a 1σ (68%) confidence level. The statistical uncertainties were insignificant compared to the systematic uncertainty, except near threshold, the latter of which was estimated to be about 7%: beam current integration (3%), detector efficiency (5%), counting geometry (1%), decay corrections (2%) and target thickness (3%).

3 Results and discussion

The measured ^{28}Mg thick-target production rate curve for NaCl + p is shown in figure 1. (Note that all target materials considered in this study are natural, non-enriched materials. The relatively high proton energies will make the correspondingly thick targets required prohibitively expensive should enriched target material be used.) The reaction threshold is near 50 MeV and the production rate for the full energy region, i.e., from threshold up to 200 MeV, is about 6 MBq/μAh. A standard polynomial function was fitted through the measured data using the code TableCurve [14].

The polynomial of figure 1 could be differentiated analytically, allowing the derivation of the excitation function for ^{nat}Cl + p, shown in figure 2. (Note that this excitation function pertains to pure Cl and not NaCl.) The only other relevant data found in the literature are by Lundqvist and Malmborg [15], which currently is the only EXFOR data set for ^{28}Mg produced in ^{nat}Cl + p. Six of their nine values are in good agreement with our present results, while three values are clearly somewhat higher. Generally, the agreement is satisfactory. The deduced cross section values of this work are presented in table 1.

Lundqvist and Malmborg [15] presented production cross sections for ^{28}Mg in the proton bombardment of silicon, phosphorus, sulphur, chlorine, argon and potassium. These were essentially all the possible target elements with potential in the energy region 50–180 MeV. The target materials and reactions are as follows: Si [^{30}Si(p,3p)^{28}Mg]; $Na_2P_2O_7$ [^{31}P(p,4p)^{28}Mg]; Na_2SO_4 [^{nat}S(p,5pxn)^{28}Mg]; LiCl [^{nat}Cl(p,6pxn)^{28}Mg]; Ar [^{nat}Ar(p,7pxn)^{28}Mg]; and K_2CO_3 [^{nat}K(p,8pxn)^{28}Mg]. From a practical targetry point of view,

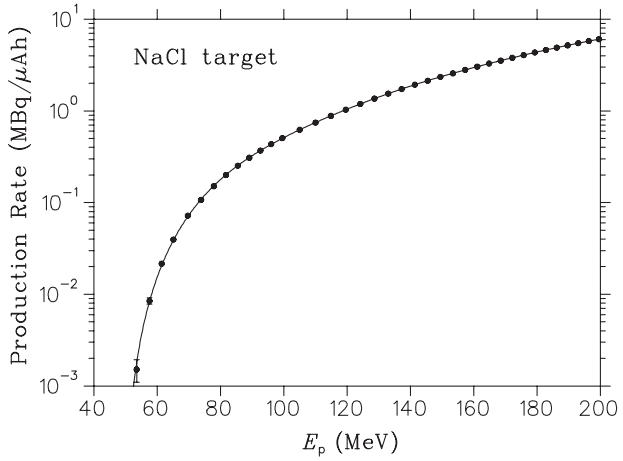

Fig. 1. Thick-target production rate curve of ^{28}Mg produced in the proton bombardment of NaCl. The solid symbols are the measured values of this work while the solid curve is a polynomial fit. Error bars are shown when they exceed the symbol size.

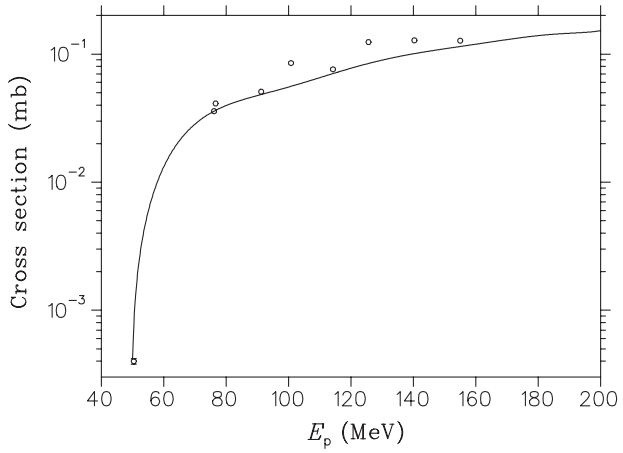

Fig. 2. Excitation function of ^{28}Mg formed in the reactions of protons with ^{nat}Cl. The solid curve was derived from the measured thick-target production rate data of this study (see fig. 1). The open symbols are measured cross sections by Lundqvist and Malmborg [15].

one can omit Ar. As a gas, Ar will be impossible to contain in a large enough energy window to make ^{28}Mg production viable, while it is impractical to keep it frozen under high-intensity bombardment conditions. One can also omit Si, S and K, as with these elements, significantly lower cross sections were obtained than with Cl and P. Interestingly, the ^{nat}P + p process has higher cross sections for ^{28}Mg formation than ^{nat}Cl + p (about 30% at 150 MeV). Unfortunately, no suitable compounds of P could be identified for use as target material, as they all seem to have poor thermal stability at higher temperatures and/or a relatively low P content. Many phosphorus compounds decompose at relatively low temperatures, rendering them unsafe as target materials. One of the most stable compounds of P namely $Na_4P_2O_7$ (sodium pyrophosphate) has, for example, a reasonably high melting point of 880 °C but only contains 23% of P by mass. In contrast, many of the chlorides have excellent thermal properties and a high Cl content. Several chlorides have boiling points at temperatures much higher than their melting points, thus making excellent

high-current targets if properly encapsulated and cooled. Also, both stable isotopes of Cl contribute significantly to the yield: ^{35}Cl[75.77%](p,6p2n)^{28}Mg and ^{37}Cl[24.23%](p,6p4n)^{28}Mg.

Figure 3 shows the expected thick-target production rates (or instantaneous yields) for several metal chlorides as well as pure chlorine for an energy window from threshold up to 200 MeV. Obviously, solid frozen chlorine will be the best choice in terms of yield but it is quite impractical as a target. The next best choice in terms of yield is $BeCl_2$, however, this particular salt has less favourable thermal properties than the simpler chlorides, viz. LiCl, NaCl and KCl. In our opinion, LiCl is the target material of choice, as it has excellent thermal stability as well as a yield of about 80% of the ^{nat}Cl + p theoretical maximum. LiCl has a melting point of 605 °C and a boiling point of 1325 °C, while the corresponding values for $BeCl_2$ are 405 °C and 488 °C, respectively. It also gives a 37% higher ^{28}Mg yield than NaCl.

Once again, however, this is not the complete story as a production energy window of 50–200 MeV will result in a very thick LiCl target (about 32 g/cm^2). Such a thick target is virtually impossible to cool sufficiently during high-intensity irradiation. A practical solution is to place several thinner targets (properly encapsulated) in series and to provide fast flowing cooling water in a 4π geometry [16]. This will reduce the cumulative production rate somewhat by introducing dead layers in the production energy window. Nevertheless, a higher operational beam intensity can more than adequately compensate for this loss.

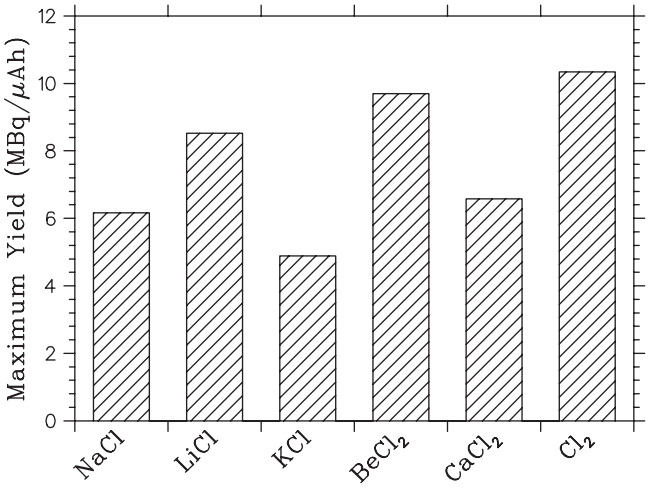

Fig. 3. Comparison of the expected thick-target production rates of ^{28}Mg in the proton irradiation of several Cl containing compounds, for an energy window 50–200 MeV, derived from the measured data of this work.

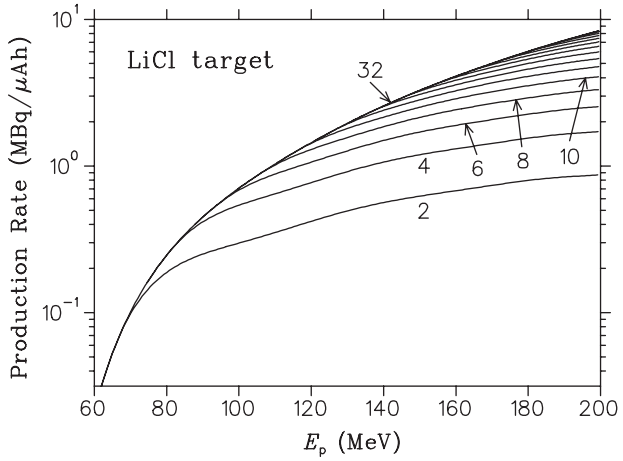

Fig. 4. Expected production rates of ^{28}Mg for various target thicknesses in the proton irradiation of LiCl, plotted as a function of incident energy. The target thicknesses range from 2 g/cm^2 to 32 g/cm^2 in 2 g/cm^2 steps, as indicated.

Table 1. Cross sections for the production of ^{28}Mg in ^{nat}Cl + p. These values were deduced from the thick-target production rate measurements on NaCl (see text).

Proton energy (MeV)	Cross section ± Error (μb)
50	0.41 ± 0.07
55	5.9 ± 0.5
60	13.2 ± 0.9
65	21.1 ± 1.5
70	28.4 ± 2.0
75	34.6 ± 2.4
80	39.6 ± 2.8
85	43.8 ± 3.1
90	47.4 ± 3.3
100	55.3 ± 3.9
105	60.0 ± 4.2
110	65.4 ± 4.6
115	71.3 ± 5.0
120	77.5 ± 5.4
125	83.7 ± 5.9
130	89.7 ± 6.3
135	95.3 ± 6.7
140	100.4 ± 7.0
145	105.2 ± 7.4
150	109.9 ± 7.7
155	114.5 ± 8.0
160	119.4 ± 8.4
165	124.4 ± 8.7
170	129.7 ± 9.1
175	134.7 ± 9.4
180	139.2 ± 9.7
185	142.8 ± 10.0
190	145.3 ± 10.2
195	147.6 ± 10.3
200	152.3 ± 10.7

It is interesting to compare the yields expected from thinner targets as a function of incident energy. This is shown in figure 4 for LiCl targets ranging in thickness from 2 g/cm^2 to 32 g/cm^2. It is clear that, regardless of the target thickness, the highest yield is always obtained with the highest incident proton energy. There are no local minima or maxima. The production rate values at an incident energy of 200 MeV is shown in figure 5 as a function of target thickness.

At our laboratory, we tested salt targets of 4 g/cm^2 thickness and 20 mm in diameter, encapsulated in 0.5 mm thick Al, successfully up to thermal loads of 2.5 kW. Cooling water

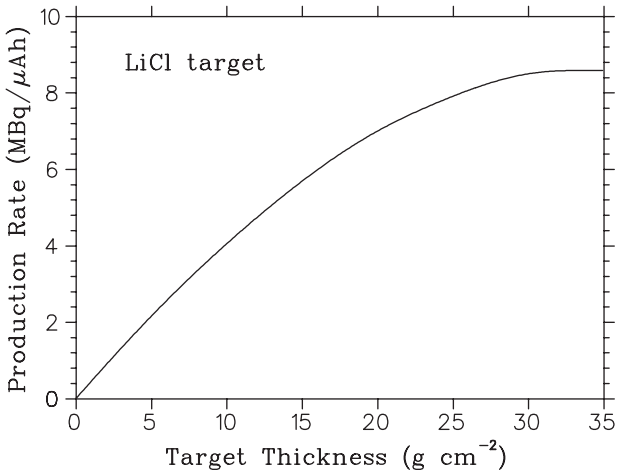

Fig. 5. Expected thick-target production rates of ^{28}Mg in the proton irradiation LiCl with an incident energy of 200 MeV, plotted as a function of target thickness.

layers of 1 mm thickness were provided to targets having a tandem geometry. This concept can easily be extended to more targets in series. Table 2 summarizes such a scheme. Note that a yield of 89.2% of the theoretical maximum for LiCl + p over the energy region from threshold up to 200 MeV can be obtained by having 7 such targets in series. With 5 targets, this value is nearly 80% and, perhaps, a good compromise from a practical perspective.

Table 2. Production details of a series of Al-encapsulated LiCl targets of 4 g/cm^2 thickness, separated by 1 mm thick water layers for cooling (see text). The incident proton beam energy is 200 MeV.

Target	Energy window (MeV)	Production rate (MBq/μAh)	% Theor. max.	% Cumulative
1	198.0 – 183.6	1.71	20.3	20.3
2	182.1 – 166.8	1.58	18.8	39.1
3	165.2 – 148.8	1.37	16.3	55.4
4	147.0 – 129.1	1.15	13.7	69.1
5	127.2 – 107.0	0.88	10.5	79.6
6	104.9 – 81.0	0.59	7.0	86.6
7	78.3 – 45.9	0.22	2.6	89.2

4 Conclusions

It is evident from the literature that a relatively low production rate is typical of all production routes for ^{28}Mg. Useful quantities can, nevertheless, be produced with proton-induced reactions, provided that a sufficiently high incident beam energy is available. In our opinion, LiCl is the target material of choice for the energy region 50–200 MeV. The nuclear data measured for ^{nat}Cl + p as part of this study were employed to calculate the expected production rate for a practical target arrangement, using several encapsulated salt targets in series. It was shown that provision can be made for proper cooling while still retaining a high percentage of the theoretical maximum yield.

The excitation function of ^{28}Mg in the reaction ^{nat}Cl + p was not measured in the usual way, i.e. by means of the stacked-foil technique, due to difficulties experienced in making thin specimens of a brittle target material. Instead, it was deduced from the thick-target production rate curve, which was experimentally determined by irradiating thick targets. This method may, in other similar cases, be an appropriate alternative to the stacked-foil technique.

References

1. R.K. Sheline, K. Johnson, Phys. Rev. **89**, 520 (1953).
2. J.K. Aikawa, G.S. Gordon, E.L. Rhoades, J. Appl. Physiology **15**, 503 (1960).
3. M. Verhas, V. de la Gueronniere, J.M. Grognet, J. Paternot, A. Hermanne, P. van den Winkel, R. Gheldof, P. Martin, M. Fantino, Y. Rayssiguier, Eur. J. Clinical Nutrition **56**, 442 (2002).
4. T. Bohn, *Magnesium Absorption in Humans*, Thesis, Diss. ETH No. 14930, University of Frankfurt, Germany, 2003, and references therein.
5. R. Schwartz, E.M. Wien, R.A. Wentworth, J. Nutr. **111**, 219 (1981).
6. M.L. Heijnen, G.J. van den Berg, A.C. Beynen, J. Nutr. **126**, 2253 (1996).
7. Z.I. Kolar, J.A. van der Velden, R.C. Vollinga, P. Zandbergen, J.J.M. de Goejj, Radiochim. Acta **54**, 167 (1991), and references therein.
8. R. Michel, R. Bodemann, H. Busemann, R. Daunke, M. Gloris, H.-J. Lange, B. Klug, A. Krins, I. Leya, M. Luepke, S. Neumann, H. Reinhardt, M. Schnatz-Buettgen, U. Herpers, T. Schiekel, F. Sudbrock, B. Holmqvist, H. Conde, P. Malmborg, M. Suter, B. Dittrich-Hannen, P.-W. Kubic, H.-A. Sinal, D. Filges, Nucl. Instrum. Meth. B **129**, 153 (1997).
9. R. Iwata, M. Kawamura, T. Ido, S. Kimura, J. Radioanal. Nucl. Chem. **159**, 233 (1992).
10. H.J. Probst, S.M. Qaim, R. Weinreich, Appl. Radiat. Isot. **27**, 431 (1976).
11. S.M. Qaim, Radiochim. Acta **30**, 147 (1982).
12. K. Gul, A. Hermanne, M.G. Mustafa, F.M. Nortier, P. Obložinský, S.M. Qaim, B. Scholten, Y. Shubin, S. Takács, F.T. Tárkányi, Z. Zhuang, *Charged particle cross-section database for medical radioisotope production: diagnostic radioisotopes and monitor reactions*, IAEA-TECDOC-1211, IAEA, Vienna, May 2001. Available from URL: http://www-nds.iaea.org/medical/. (last updated 2005).
13. R.B. Firestone, L.P. Ecktröm, WWW Table of Radioactive Isotopes, Version 2.1, January 2004. Available from URL: http://ie.lbl.gov/toi.
14. TABLECURVE 2D Automated Curve Fitting & Equation Discovery, Jandel Scientific, San Rafael, California, 1996.
15. H. Lundqvist, P. Malmborg, Appl. Radiat. Isot. **30**, 33 (1979).
16. F.M. Nortier, F.J. Haasbroek, S.J. Mills, H.A. Smit, G.F. Steyn, C.J. Stevens, T.F.H.F. van Elst, E. Vorster, *Targetry for the routine bombardment of solid targets at the National Accelerator Centre*, in *Proc. 4th Int. Workshop on Targetry and Target Chemistry*, *PSI, Villigen, Switzerland 9–12 Sept. 1991*, edited by R. Weinreich, PSI-Proceedings 92-01 (1992).